ARTICLE

doi:10.1038/nature09733

Evolution of human *BCR–ABL1* lymphoblastic leukaemia-initiating cells

Faiyaz Notta[1,2]*, Charles G. Mullighan[3]*, Jean C. Y. Wang[1,4], Armando Poeppl[1], Sergei Doulatov[1,2], Letha A. Phillips[3], Jing Ma[5], Mark D. Minden[4], James R. Downing[3] & John E. Dick[1,2]

Many tumours are composed of genetically diverse cells; however, little is known about how diversity evolves or the impact that diversity has on functional properties. Here, using xenografting and DNA copy number alteration (CNA) profiling of human *BCR–ABL1* lymphoblastic leukaemia, we demonstrate that genetic diversity occurs in functionally defined leukaemia-initiating cells and that many diagnostic patient samples contain multiple genetically distinct leukaemia-initiating cell subclones. Reconstructing the subclonal genetic ancestry of several samples by CNA profiling demonstrated a branching multi-clonal evolution model of leukaemogenesis, rather than linear succession. For some patient samples, the predominant diagnostic clone repopulated xenografts, whereas in others it was outcompeted by minor subclones. Reconstitution with the predominant diagnosis clone was associated with more aggressive growth properties in xenografts, deletion of *CDKN2A* and *CDKN2B*, and a trend towards poorer patient outcome. Our findings link clonal diversity with leukaemia-initiating-cell function and underscore the importance of developing therapies that eradicate all intratumoral subclones.

A widely accepted tenet of cancer biology is that most tumours arise from single cells and that multiple genetic alterations accumulate over time, resulting in transformation[1]. Historically, this process was considered to be a stepwise acquisition of new mutations, some of which provide a competitive growth advantage, resulting in successive rounds of clonal expansion with concomitant loss of earlier, less-fit clones[2]. In this model of tumour evolution, all clones are linearly related to each other. However, new genomic technologies are revealing a more complex clonal architecture in some cancers[3–6]. Analysis of chromosomal translocation breakpoints and CNA profiling in twins with *ETV6–RUNX1*-positive acute lymphoblastic leukaemia (ALL) showed that a pre-leukaemic clone is initiated *in utero* that expands, seeds both twins, and then evolves with different kinetics and CNA acquisition in each twin[7,8]. Genome-wide CNA profiling of paired diagnostic and relapse ALL samples has been particularly informative[9–11]. In most cases, the relapse clone shared only limited genetic identity with the predominant diagnostic clone and did not evolve from it. In the rest, the relapse clone was either identical or a direct evolutionary product of the diagnostic clone. These studies predicted the existence of an ancestral, pre-diagnostic clone that gave rise to at least two clonal lineages that evolved independently in many patients with ALL, with each clone acquiring different genetic aberrations: one clone giving rise to the dominant diagnostic clone and the other emerging as the predominant clone at relapse with the acquisition of additional CNA. These results indicate that tumour evolution may occur through a more complex branching model that gives rise to genetically distinct subclones at diagnosis that vary in aggressiveness and response to therapy[12]. However, proof of this model requires studies directly examining the functional properties of the cells in which genetic changes are found. Indeed, within leukaemias, non-proliferating or pre-apoptotic cells are often present and thus incapable of contributing to long-term clonal maintenance or to relapse. Therefore, functional studies of the cells responsible for driving leukaemic growth in patients must be combined with genetic approaches to identify genetically diverse subclones and their evolutionary ancestral precursors, and to show whether they possess biologically distinct growth properties.

Arguably the most important biological function a cancer cell can have is the ability to sustain clonal growth[13], a property best measured by tumour initiation assays in primary and secondary recipients. Indeed, some highly aggressive or metastatic tumours of mice and humans seem to be functionally homogeneous because almost every cell has tumour-initiating-cell capacity. However, most tumours appear to be functionally heterogeneous, as the tumour-initiating cells or leukaemia-initiating cells typically represent a minor fraction, although their frequency varies widely in syngeneic[14] or xenograft[15] recipients. It has been widely considered that intratumoral functional heterogeneity results from stochastic processes that influence cell growth but also from the variable behaviour of genetic subclones that arise through clonal evolution. The cancer stem cell model proposes an alternative explanation based on the hierarchical organization of the tumour clone where cancer stem cells are solely responsible for driving clonal growth and for therapeutic resistance. In the cancer stem cell model, tumour-initiating cells and cancer stem cells are synonymous and have the properties of self-renewal and maturation that are canonical to all stem cells. Epigenetic or developmental programs contribute to functional differences between cancer stem cells and non-cancer stem cells within a tumour clone that the model assumes would be genetically identical[13,16]. The cancer stem cell and clonal evolution models are the subject of intense debate and often considered to be mutually exclusive[16,17]. The cancer stem cell model focuses on the concept of functional heterogeneity but does not take into account tumour evolution, intratumoral genetic variation, or the existence of genetically distinct subclones. On the other hand, the clonal evolution model focuses on genetic heterogeneity without considering

[1]Division of Stem Cell and Developmental Biology, Campbell Family Institute for Cancer Research/Ontario Cancer Institute, Toronto, Ontario M5G 1L7, Canada. [2]Department of Molecular Genetics, University of Toronto, Toronto, Ontario M5G 1L7, Canada. [3]Department of Pathology, St Jude Children's Research Hospital, Memphis, Tennessee 38105, USA. [4]Department of Medical Oncology and Hematology, Princess Margaret Hospital, and Department of Medicine, University of Toronto, Toronto, Ontario M5G 2M9, Canada. [5]Hartwell Center for Bioinformatics and Biotechnology, St Jude Children's Research Hospital, Memphis, Tennessee 38105, USA.
*These authors contributed equally to this work.

the functional variation that might exist intratumorally within individual genetic subclones. As a first step to resolve the basis for intratumoral heterogeneity, functional assays must be combined with genetic analysis to determine whether tumours contain genetically distinct subclones of tumour-initiating cells.

Philadelphia chromosome acute lymphoblastic leukaemia (Philadelphia-positive (Ph^+) ALL) is an ideal disease in which to study the relationship between intratumoral clonal diversity, genetic alterations and cellular growth properties because it is considered a single clinical entity with identifiable and recurrent genetic abnormalities. Detailed studies have revealed a number of genetic alterations, notably deletions of the lymphoid transcriptional regulator *IKAROS* (also called *IKZF1*), *PAX5*, *EBF1*, as well as deletions involving *CDKN2A/B* that cooperate with *BCR–ABL1* in lymphoid leukaemogenesis[18]. Furthermore, the association of *IKZF1* deletion in Ph-negative ALL with poor patient outcome predicts that it will be possible to link specific genetic alterations with function[19]. Here we report development of a robust Ph^+ ALL xenograft system that was used to carry out a combined genetic and functional study of the genetic diversity of functionally defined tumour-initiating cells derived from diagnostic patient samples.

Modelling human Ph^+ ALL in xenografts

To determine whether a single genetic subtype of leukaemia like Ph^+ ALL exhibits uniform growth properties, we used three xenograft models of increasing immune deficiency: NOD.CB17-*Prkdc*^{scid}/J (NOD/SCID) mice; NOD/SCID mice treated with anti-CD122 to deplete innate immune cells (NS122)[20,21]; or NOD/SCID mice with deletion of the common gamma (γ)-chain (NSG)[22] (Supplementary Fig. 1). Diagnosis samples from 18 of 20 Ph^+ ALL patients efficiently engrafted NS122 mice (Supplementary Fig. 2) and recapitulated numerous aspects of the human disease including tumour dissemination, immunophenotype (Supplementary Fig. 3) and morphology (Supplementary Fig. 4). However, 10 of 20 patient samples caused clinically manifest disease before 15 weeks and were categorized as aggressive group 1 samples, whereas the remaining xenograft mice appeared healthy until they were killed and these were classified as non-aggressive group 2 samples (Fig. 1a). Accordingly, the leukaemic burden in bone marrow and systemic dissemination was significantly higher in group 1 versus group 2 samples (Fig. 1b, c, Supplementary Fig. 2b and Supplementary Table 1). Notably, group 1 samples engrafted all recipient types (Fig. 1d and Supplementary Fig. 5) even when transplanted at near-limiting dose (Supplementary Fig. 6). By contrast, group 2 samples failed to engraft to NOD/SCID mice (Fig. 1d and Supplementary Fig. 5) despite injection of 50-fold more cells (Supplementary Fig. 7). Of two group 2 samples (patient 2-5 and 2-6) unable to engraft NS122 recipients, one engrafted NSG mice (Supplementary Fig. 8). The extent of leukaemic dissemination was similar in NS122 or NSG mice for both group 1 and group 2 samples, although NSG mice had higher peripheral engraftment levels (Supplementary Fig. 9).

Genetic basis of functional heterogeneity

To examine a possible genetic basis for the distinct xenograft growth properties between group 1 and group 2 samples, genome-wide CNA profiling was undertaken. Overall, the frequency of genetic alterations in *IKZF1* (84%), *CDKN2A/B* (50%) and *PAX5* (50%) of our 20 samples paralleled previous studies[18]. A similar frequency of group 1 and group 2 samples had focal and complete deletions of the *IKZF1* locus. However, there were marked differences in the proportion with deletions of *CDKN2A/B* (group 1, 90%; group 2, 0%; $P = 0.0001$) and *PAX5* (group 1, 60%; group 2, 10%; $P = 0.057$) genes (Fig. 2e and Supplementary Table 2). Genomic quantitative polymerase chain reaction (qPCR) confirmed that the *CDKN2A/B* locus was not deleted in representative group 2 samples (Supplementary Table 3) nor hypermethylated in an independent cohort of Ph^+ ALL patients (Supplementary Fig. 10).

Because previous studies have reported a positive association between the efficiency of xenograft engraftment and clinical outcome in acute myeloid leukaemia (AML) patients[23], we compared the survival of group 1 and group 2 samples. We found a trend towards poorer outcome of group 1 patients with increased early relapse, although significance was not reached owing to the small sample number (Fig. 2f, $P = 0.08$). Limiting dilution analyses (LDA) of 11 patient samples showed that the leukaemia-initiating-cell frequency in group 1 samples was 80-fold higher than group 2 samples (Fig. 2g). The leukaemia-initiating-cell frequency in one group 1 patient was 11%, similar to the leukaemia-initiating-cell frequency previously observed in comparable murine models[24]. Although comparison of absolute leukaemia-initiating-cell frequency in xenografts and syngeneic recipients is subject to some uncertainty[25], the relative difference between group 1 and group 2 samples is consistent with their distinct growth properties. Moreover, preliminary evidence indicates that leukaemic evolution, defined by increasingly aggressive and less restrictive xenograft growth upon serial passage, also correlates with reduced functional heterogeneity as reflected by increased leukaemia-initiating-cell frequency (Supplementary Fig. 11 and Supplementary Table 4). Collectively, we provide the first data linking engraftment properties and leukaemia-initiating-cell frequency to both specific genetic events in cancer and clinical outcome of patients.

Clonal dynamics of Ph^+ ALL pathogenesis

Despite widespread use of tumour xenografts, there are few studies comparing genetic alterations in primary samples versus xenografts[6]. To determine whether genetic abnormalities of the diagnostic sample are propagated upon transplantation, we tracked the clonal dynamics of ALL growth in xenografts by comparing CNA profiles of 12 diagnosis samples (eight group 1 and four group 2 tumours) with paired primary and secondary xenografts (Fig. 2a). Overall, xenografts did not select for a specific genotype as no single lesion was acquired by all tumours (Supplementary Fig. 12 and Supplementary Table 5). In six samples, five of which were group 1, xenografts exhibited the same distribution of CNA as the diagnostic patient sample, and detailed analysis of the antigen receptor (AgR) loci confirmed that the predominant clone present at diagnosis was propagated in xenografts (Supplementary Fig. 13).

By contrast, multiple xenografts derived from the six other patient samples (three group 1 and three group 2) harboured distinct genetic changes compared to the predominant diagnostic clone (Fig. 2b, c and Supplementary Fig. 14), while also sharing major CNA such as *IKZF1* and *CDKN2A/B* (data not shown). The presence of multiple xenograft recipients from the same patient sample with both identical and new CNA strongly indicates the existence of subclones, present at low levels in the diagnostic sample, that harbour additional genetic alterations. Although these CNA are newly emergent, we could detect them in other diagnostic samples, pointing to their clinical relevance (Supplementary Fig. 12). Our findings mirror recent CNA analysis of matched diagnosis and relapse ALL patient samples where the majority of relapsed cases represent the evolution of a new clone that is related to, but distinct from, the predominant diagnostic clone[11]. Notably, the clinical outcome of patients in whom the predominant clone at diagnosis was propagated in xenografts (CNA concordant) was different from patients where xenografts were engrafted with a minor subclone that outcompeted the predominant clone (CNA discordant). CNA concordant samples had poorer outcome even within our very small cohort (Fig. 2d). These data point to the need for larger validation studies and they indicate that genetic alterations, which lead to clonal predominance at diagnosis and competitive growth advantage in xenografts, are linked to poor survival.

To determine whether the detection of minor subclones might be hindered by out-competition in xenografts of dominant or aggressive clones, we analysed the CNA profiles of two patient samples transplanted at limiting (to engraft single leukaemia-initiating cells) and at non-limiting cell doses. In patient 1-8, non-limiting (bulk) cell doses

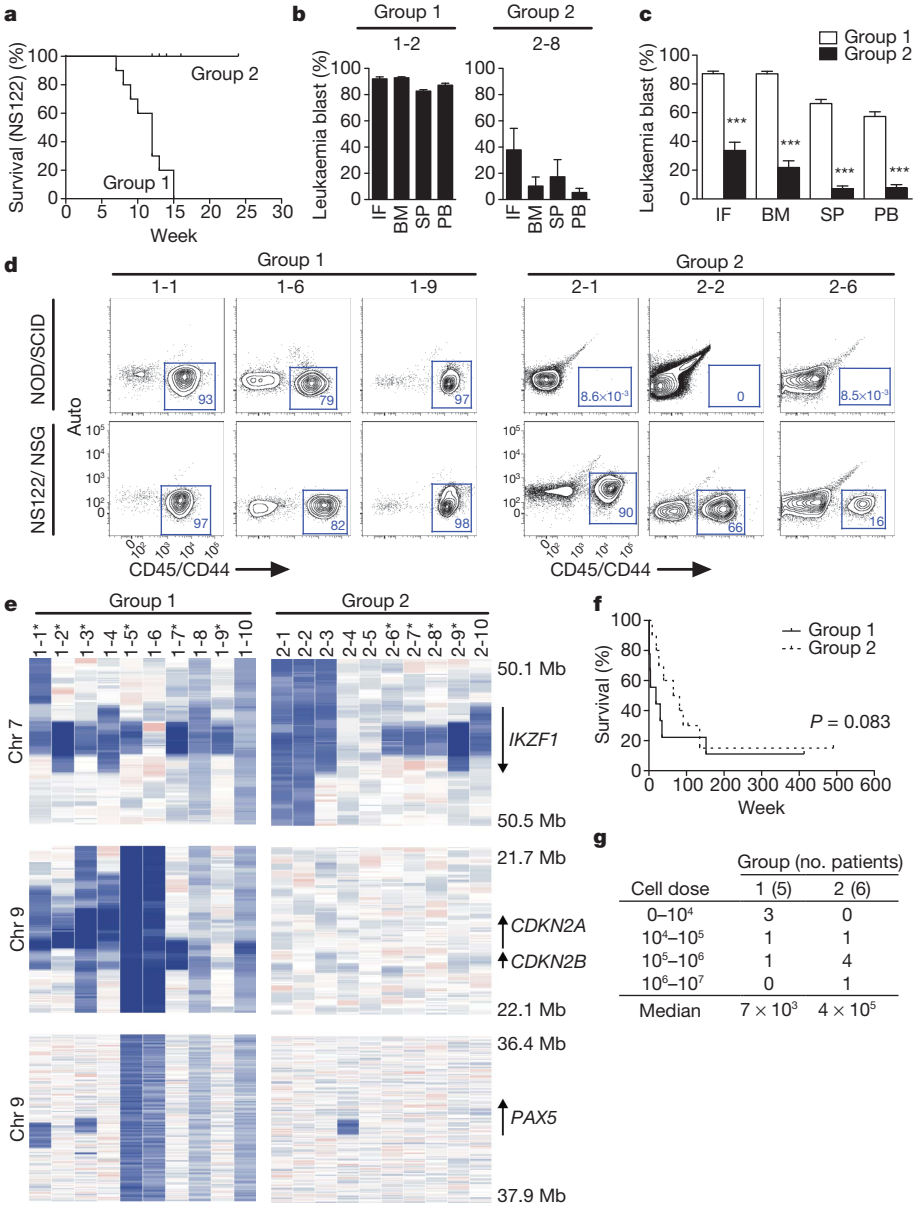

Figure 1 | Functional and genetic analysis of Ph$^+$ ALL. **a**, Survival of NS122 mice transplanted with 20 diagnostic Ph$^+$ ALL samples. Xenografts moribund before 15 weeks were categorized as group 1 (10 patient samples; $n = 90$) and the remainder that appeared healthy until they were killed for analysis were group 2 (10 patient samples; $n = 45$). **b**, Leukaemic burden in two representative patient samples, 1-2 and 2-8, determined by flow cytometry of the injected femur (IF), bone marrow (BM, left femur/tibiae), spleen (SP) and peripheral blood (PB) ($n = 4$ mice per sample; error bars, mean ± s.e.m.). **c**, Cumulative leukaemia engraftment in xenografts from panel **a** transplanted with group 1 and group 2 samples (error bars, mean ± s.e.m.; $^{***}P < 0.0001$). **d**, Comparison of leukaemic engraftment of group 1 ($n = 3$) and group 2 ($n = 3$) samples in NOD/SCID or NS122/NSG recipients. Human CD45 or CD44 (Supplementary Fig. 18) was used to evaluate chimaerism. **e**, CNA analysis of individual group 1 and group 2 patient samples using Affymetrix 6.0 SNP arrays. Regions containing *IKZF1* (top panel), *CDKN2A/B* (middle panel) and *PAX5* (bottom panel) deletions are shown. Asterisks indicate focal deletions in *IKZF1* involving exons 3–6, consistent with formation of dominant-negative *IKAROS* isoform IK6. Data are $\log_2$ ratio, median smoothing format (blue, deletion; white, normal; red, gain). See Supplementary Note for patient 1-8. **f**, Survival analysis of group 1 and group 2 patients ($P = 0.083$). **g**, Minimum cell dose required for leukaemia initiation in NS122 and NSG recipients from group 1 ($n = 5$) versus group 2 ($n = 6$) patient samples.

generated xenografts that differed at three major CNA compared to the patient sample (chromosome (Chr) 1 gain, Chr 8p deletion and Chr 8q gain) (Fig. 2e). Xenografts derived from limiting cell doses (clonal) differed from both non-limiting xenografts (lacked Chr 1 gain and 8p deletion) and the patient sample (Chr 8q gain) (Fig. 2e, m6). Patient sample 1-1 was highly aggressive in xenografts. All recipients of non-limiting cell doses and one from the limiting dose group contained the major diagnostic clone distinguished with a bi-allelic loss of *CDKN2A* (Fig. 2f, Chr 9). The other recipient from the limiting dose group did not have this CNA but retained the larger flanking CNA (Fig. 2f and Supplementary Fig. 15, m2). The topography of this lesion from each clone, together with the similarity of AgR regions in all recipients (Fig. 2e, f, top panels), indicates common genetic ancestry. Each clone remained stable after secondary transplantation (Supplementary Fig. 16). Thus, our data provide formal evidence that ALL is composed of genetically distinct subclones that are present in varying proportions at diagnosis and have differing functional capacity in xenografts. Furthermore, our analysis reveals the sequence of genetic events that probably occurred in these patients and provides unique insight into the evolution of clonal diversity during ALL leukaemogenesis.

Multi-clonal model of Ph$^+$ ALL pathogenesis

To gain an insight into the evolutionary processes that underlie the generation of dominant and minor subclones, we combined functional

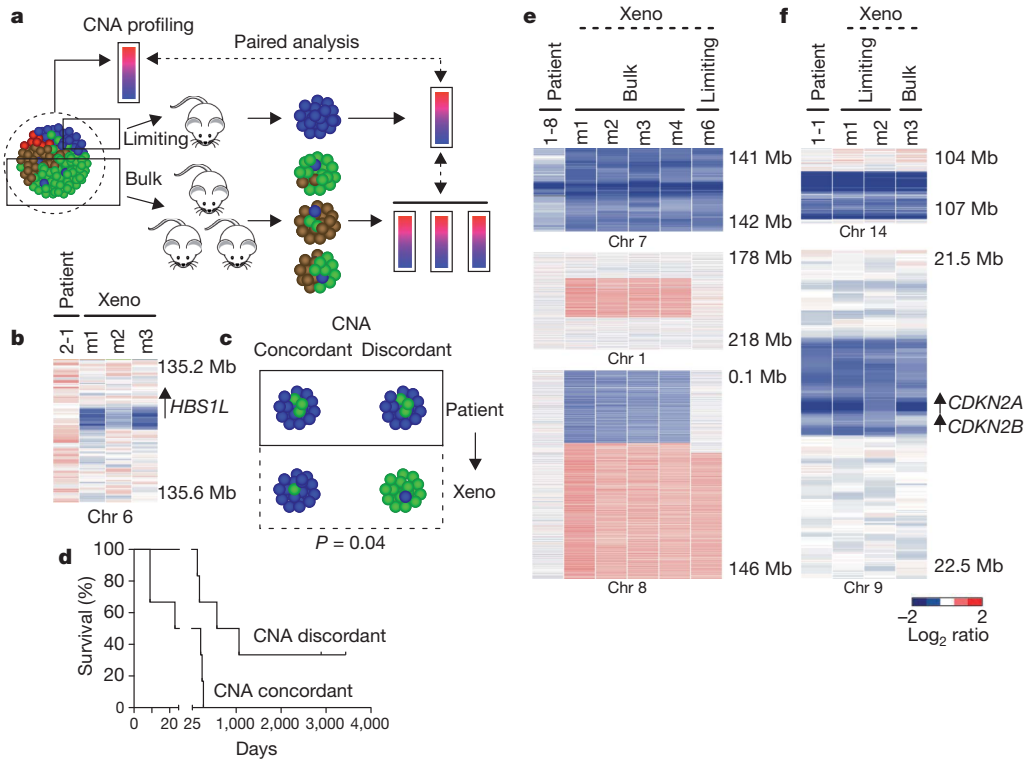

Figure 2 | Clonal dynamics of Ph$^+$ ALL upon transplant into xenografts. **a**, Schema of experimental design for tracking primary leukaemia clones in xenografts using limiting and bulk cell doses. **b**, Representative patient sample displaying a new CNA in each of three xenografts in the *HBS1L* locus that was below SNP array detection limit in the patient sample (additional examples on five patients in Supplementary Fig. 14). **c**, Pictorial representation of outgrowth of subclones (CNA discordant) or recapitulation of the predominant diagnostic clone (CNA concordant) after transplant into xenografts. **d**, Survival of patients that generated CNA concordant and discordant xenografts. **e**, **f**, CNA profiling of xenografts transplanted with limiting and bulk doses of patient cells. In patient 1-8 (**e**), multiple CNA present on Chr 1 (middle) and Chr 8 (bottom) were detected in all recipients (m1–m4) at bulk cell doses (1×10^6 per mouse) that were not detected in the diagnostic sample. At limiting cell dose, one of three mice was engrafted (5,000 cells per mouse, m6) and had partial similarity to the other bulk recipients (Chr 7 AgR deletion, top panel; Chr 8q gain, bottom panel) and the diagnostic sample (Chr 7, AgR deletion). In patient 1-1 (**f**), two of nine mice were engrafted at limiting cell doses (50 cells per mouse; m1, m2) and a single recipient at non-limiting cell dose ($\sim 1 \times 10^6$ cells; m3). The diagnostic sample, m1 and m3 share common CNA in *CDKN2A*, not present in m2 (bottom panel). All samples share common CNA at the AgR locus (top panel). Data are $\log_2$ ratio, median smoothing format (blue, deletion; white, normal; red, gain).

analysis obtained from xenografts with clonal analysis carried out by CNA profiling on multiple xenografts derived from a group 1 and group 2 sample. For both patient samples, the dominant diagnostic was not detected in xenografts, rather they were repopulated with several related but distinct genetic subclones. Detailed tracking of CNA provided an unprecedented opportunity to gain an insight into the sequence of lesion acquisition in independent subclones. For example, in patient 1-6, deletion of the AgR region of Chr 11 in all recipients indicates that this change was an early event in disease pathogenesis that was shared by all subclones that outgrew after transplant, followed by a gain in a region of Chr 6q present in leukaemic cells from two xenografts or a deletion at the Chr 14 immunoglobulin heavy chain (*IGH*) locus in a different subclone found in another xenograft (Fig. 3a). Patient 2-9 displayed a CNA (gain) in Chr Xp (Fig. 3b, Chr X) at diagnosis. All xenografts displayed varying loss of this region, indicating that this CNA was acquired early in pathogenesis of this patient sample. Only two recipients contained a subsequent Chr 9q deletion (m37 and m39), with further clonal divergence leading to a deletion in a region of Chr 8q (seen in m37) and duplication of Chr 8q (seen in m39) (Fig. 3b, Chr 8 and 9). Interestingly, xenograft m41 also displayed duplication in Chr 8q, but lacked a deletion in chromosome 9. Therefore, it remains unclear which CNA (Chr 9 deletion or Chr 8q duplication) was acquired first in the patient. Data are summarized pictorially for both patient samples (Fig. 3, right panel). These data indicate that multiple tumour clones coexist in the diagnostic patient sample, and that these clones undergo divergent evolution from the diagnostic clone, supporting the branching model of tumour progression[12].

Intratumoral heterogeneity may promote clonal evolution by increasing the number of selectable traits under any given stress. Therefore, genetic diversification is probably important for tumour survival. Recently, the degree of genetic diversification has been linked to clinical aggressiveness of breast tumours[26], and is associated with metastasis in pancreatic cancer[4,5]. To determine whether the various subclones we identified in patient sample 1-6 could evolve further, two primary xenografts were transplanted into secondary recipients. All CNA from primary xenografts were detected in secondary recipients, indicating overall stability of each subclone (Supplementary Fig. 17a). However, new CNA were detected in three of nine recipients, indicating that ongoing evolution and further progression of disease can occur, although it seems to be largely stochastic (Supplementary Fig. 17b). Although limiting dilution studies were not performed to completely rule out the possibility that additional minor subclones, undetected in the primary xenograft, contributed to these new CNA, these data indicate that genetic diversification can continue in the xenograft.

Discussion

Here we establish that individual Ph$^+$ ALL samples at diagnosis are composed of genetically diverse subclones that are related through a complex evolutionary process. These subclones vary in their xenograft growth properties and leukaemia-initiating-cell frequency. Furthermore, Ph$^+$ ALL patient samples can be segregated into two subgroups on the basis of functional xenograft growth properties and specific genetic mutations. The group that lost *CDKN2A/B* and had a tendency to poorer

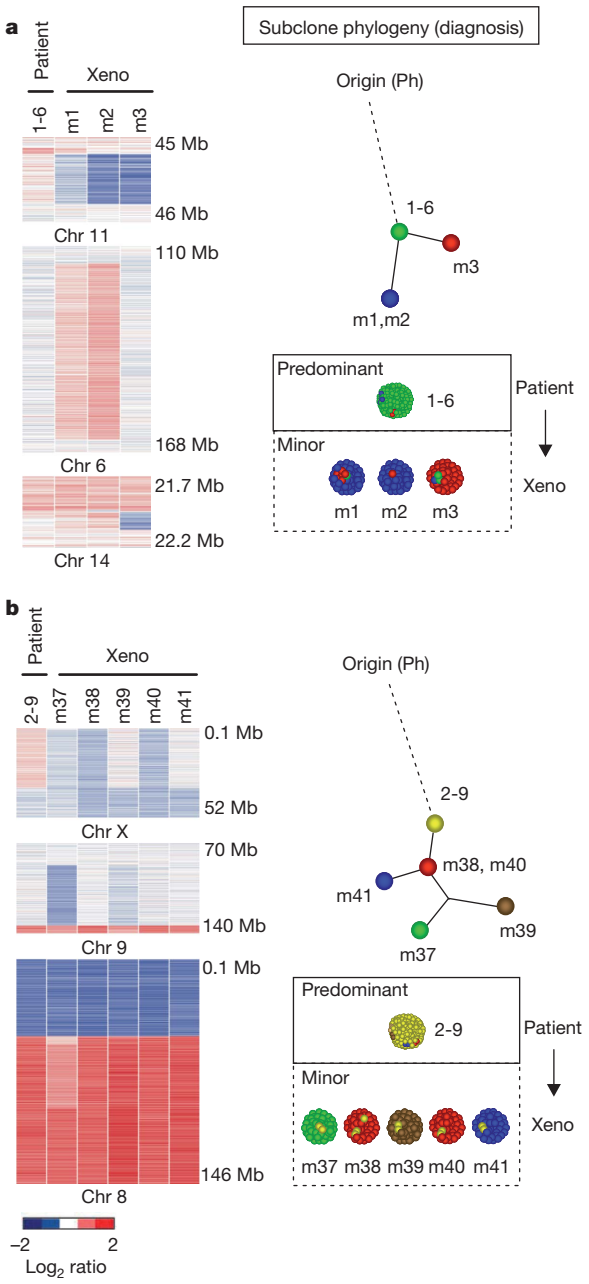

Figure 3 | Detection of genetically diverse leukaemia-initiating cells in Ph$^+$ ALL. **a**, CNA profiling shows that three engrafted recipients from sample 1-6 share a common CNA on Chr 11 (top) that is not detected in the diagnostic sample, but each is distinct for CNA on Chr 6 (middle) and Chr 14 (bottom). **b**, In sample 2-9, all five engrafted recipients shared a deletion (at varying degrees) in a region of Chr Xp (top), two recipients displayed a common CNA region of Chr 9q (middle; m37, m39), and three recipients had deletions (m37) and duplications (m39, 41) on regions of Chr 8p (bottom). A phylogenetic tree depicting the relationship between major and minor genetic subclones present in the diagnostic sample and a summary of the distinct xenograft subclones are shown to the right of each sample. The dashed line represents clonal evolution from disease origin (Ph, Philadelphia chromosome).

survival correlated with aggressive dissemination in xenografts and higher leukaemia-initiating-cell frequency. These results are consistent with the aggressive, tyrosine-kinase-inhibitor-resistant Ph$^+$ ALL seen in murine models where *Cdkn2a* is lost. The discovery that, at diagnosis, genetically distinct samples and subclones already possess variably aggressive growth properties points to the need to develop effective therapies to eradicate all intratumoral genetic subclones to prevent further evolution and recurrence. The ability to segregate even minor subclones in xenografts is a powerful tool for the preclinical development of new therapeutic strategies.

The segregation of individual genetic subclones in xenografts provided an opportunity to reconstruct the functional genetic ancestry of subclones present in diagnostic samples. Our data illustrate that leukaemic progression can occur in either a linear or branching fashion, with multiple genetic subclones evolving either in succession or in parallel, respectively. The xenograft growth characteristics of minor subclones were distinct: sometimes they out-competed the dominant clone, whereas in others (mostly group 1), they did not. The competitive advantage of the dominant clone also appeared to associate with poorer clinical outcome, although the size of the cohort was small. We speculate that some genetic events, such as loss of *CDKN2A/B*, contribute to clonal predominance at diagnosis and competitive xenograft growth. By contrast, the reduced competitive advantage of minor subclones indicates that additional genetic events are required for increased aggressiveness. However, if minor subclones survive therapy, further evolution and expansion could occur, leading to future relapse, consistent with previous genetic studies of paired diagnosis and relapse samples[11]. Because gene silencing and other epigenetic events contribute to tumour progression, our results also highlight the need for genome-wide methylation analysis of individual subclones. Evolution by branching increases subclonal complexity and underscores the importance of gaining a better molecular understanding of each subclone within a tumour.

Outgrowth of subclones in serial xenografts can only be sustained by leukaemia-initiating cells, and our findings establish that genetic diversity occurs in this functionally important cell type. Moreover, the discovery that specific genetic events influence leukaemia-initiating-cell frequency and that genetically distinct leukaemia-initiating cells evolve through a complex evolutionary process indicates that a close connection must exist between genetic and functional heterogeneity. This has several implications that may bring together the clonal evolution and cancer stem cell models. We remain cautious in extrapolating our findings in the absence of prospective isolation proving the existence of leukaemia stem cells in Ph$^+$ ALL; however, strong evidence is accumulating for the existence and relevance of leukaemia stem cells in other forms of leukaemia[27] and it is likely that genetically diverse leukaemia stem cells will eventually be found. If the leukaemia-initiating-cell/leukaemia stem cell link is established, we can speculate that leukaemia stem cells are not static but are able to evolve genetically and represent units of selection in tumour evolution. As tumours evolve, the frequency of leukaemia stem cells increases, eventually progressing to a highly advanced state that might no longer adhere to a cancer stem cell model. The high leukaemia-initiating-cell frequency that we observed in some samples and from several murine models[16,24] supports this idea. Finally, as tumours are composed of genetically diverse subclones, prospective isolation of leukaemia stem cells/cancer stem cells needs to be interpreted with considerable care, as fractionation of cancer stem cell and non-cancer stem cell populations could segregate genetically distinct subclones with variable tumour-initiating-cell capacity as opposed to genetically identical cells with differing epigenetic/developmental programs. Because the hierarchy model posits that cancer stem cells give rise to non-cancer stem cells, future studies must account for subclonal diversity and establish the genetic identity of cancer stem cells and non-cancer stem cells. Overall, our findings indicate that there may be more commonalities between clonal evolution and cancer stem cell models of cancer than previously thought and that future studies may lead to a unification of these concepts.

METHODS SUMMARY

Diagnostic Ph$^+$ ALL patient samples were intrafemorally transplanted into female NOD.CB17-*Prkdc*^{scid}/J (NOD/SCID) mice, NOD/SCID mice treated with mouse anti-CD122 (as previously described) and NOD.Cg-*Prkdc*^{scid} *Il2rg*^{tm1Wjl}/SzJ (NSG) mice. Xenograft recipients were monitored for disease sickness, and chimaerism was evaluated in various haematopoietic tissues using flow cytometry. DNA copy

number alteration (CNA) was carried out with Affymetrix 6.0 SNP arrays on the diagnostic patient sample and corresponding xenografts.

Full Methods and any associated references are available in the online version of the paper at www.nature.com/nature.

Received 10 June; accepted 3 December 2010.

1. Hanahan, D. & Weinberg, R. A. The hallmarks of cancer. *Cell* **100,** 57–70 (2000).
2. Nowell, P. C. The clonal evolution of tumor cell populations. *Science* **194,** 23–28 (1976).
3. Barrett, M. T. *et al.* Evolution of neoplastic cell lineages in Barrett oesophagus. *Nature Genet.* **22,** 106–109 (1999).
4. Campbell, P. J. *et al.* The patterns and dynamics of genomic instability in metastatic pancreatic cancer. *Nature* **467,** 1109–1113 (2010).
5. Yachida, S. *et al.* Distant metastasis occurs late during the genetic evolution of pancreatic cancer. *Nature* **467,** 1114–1117 (2010).
6. Ding, L. *et al.* Genome remodelling in a basal-like breast cancer metastasis and xenograft. *Nature* **464,** 999–1005 (2010).
7. Bateman, C. M. *et al.* Acquisition of genome-wide copy number alterations in monozygotic twins with acute lymphoblastic leukemia. *Blood* **115,** 3553–3558 (2010).
8. Hong, D. *et al.* Initiating and cancer-propagating cells in TEL-AML1-associated childhood leukemia. *Science* **319,** 336–339 (2008).
9. Li, A. *et al.* Sequence analysis of clonal immunoglobulin and T-cell receptor gene rearrangements in children with acute lymphoblastic leukemia at diagnosis and at relapse: implications for pathogenesis and for the clinical utility of PCR-based methods of minimal residual disease detection. *Blood* **102,** 4520–4526 (2003).
10. Zuna, J. *et al.* TEL deletion analysis supports a novel view of relapse in childhood acute lymphoblastic leukemia. *Clin. Cancer Res.* **10,** 5355–5360 (2004).
11. Mullighan, C. G. *et al.* Genomic analysis of the clonal origins of relapsed acute lymphoblastic leukemia. *Science* **322,** 1377–1380 (2008).
12. Greaves, M. Cancer stem cells: back to Darwin? *Semin. Cancer Biol.* **20,** 65–70 (2010).
13. Dick, J. E. Stem cell concepts renew cancer research. *Blood* **112,** 4793–4807 (2008).
14. Bruce, W. R. & Van Der Gaag, H. A quantitative assay for the number of murine lymphoma cells capable of proliferation *in vivo*. *Nature* **199,** 79–80 (1963).
15. Diehn, M., Cho, R. W. & Clarke, M. F. Therapeutic implications of the cancer stem cell hypothesis. *Semin. Radiat. Oncol.* **19,** 78–86 (2009).
16. Shackleton, M., Quintana, E., Fearon, E. R. & Morrison, S. J. Heterogeneity in cancer: cancer stem cells versus clonal evolution. *Cell* **138,** 822–829 (2009).
17. Marusyk, A. & Polyak, K. Tumor heterogeneity: causes and consequences. *Biochim. Biophys. Acta* **1805,** 105–117 (2010).
18. Mullighan, C. G. *et al.* BCR-ABL1 lymphoblastic leukaemia is characterized by the deletion of Ikaros. *Nature* **453,** 110–114 (2008).
19. Mullighan, C. G. *et al.* Deletion of *IKZF1* and prognosis in acute lymphoblastic leukemia. *N. Engl. J. Med.* **360,** 470–480 (2009).
20. McKenzie, J. L., Gan, O. I., Doedens, M. & Dick, J. E. Human short-term repopulating stem cells are efficiently detected following intrafemoral transplantation into NOD/SCID recipients depleted of $CD122^+$ cells. *Blood* **106,** 1259–1261 (2005).
21. Taussig, D. C. *et al.* Anti-CD38 antibody-mediated clearance of human repopulating cells masks the heterogeneity of leukemia-initiating cells. *Blood* **112,** 568–575 (2008).
22. Shultz, L. D. *et al.* Human lymphoid and myeloid cell development in NOD/LtSz-*scid IL2R*γ^{null} mice engrafted with mobilized human hemopoietic stem cells. *J. Immunol.* **174,** 6477–6489 (2005).
23. Pearce, D. J. *et al.* AML engraftment in the NOD/SCID assay reflects the outcome of AML: implications for our understanding of the heterogeneity of AML. *Blood* **107,** 1166–1173 (2006).
24. Williams, R. T., den Besten, W. & Sherr, C. J. Cytokine-dependent imatinib resistance in mouse $BCR\text{-}ABL^+$, Arf-null lymphoblastic leukemia. *Genes Dev.* **21,** 2283–2287 (2007).
25. Dick, J. E. Looking ahead in cancer stem cell research. *Nature Biotechnol.* **27,** 44–46 (2009).
26. Park, S. Y., Gonen, M., Kim, H. J., Michor, F. & Polyak, K. Cellular and genetic diversity in the progression of in situ human breast carcinomas to an invasive phenotype. *J. Clin. Invest.* **120,** 636–644 (2010).
27. Tehranchi, R. *et al.* Persistent malignant stem cells in del(5q) myelodysplasia in remission. *N. Engl. J. Med.* **363,** 1025–1037 (2010).

Supplementary Information is linked to the online version of the paper at www.nature.com/nature.

Acknowledgements We would like to thank S. Minkin for statistical analysis of patient outcome, the Dick Laboratory and B. Neel for critical review of this manuscript, M. Cooper for editorial assistance, and P. A. Penttilä, L. Jamieson, J. Yuan and S. Zhao for preparative flow cytometry. This work was supported by funds from Canadian Institutes for Health Research (CIHR) studentships (F.N., S.D.), the Pew Charitable Trusts (C.G.M.), The Stem Cell Network of Canadian National Centres of Excellence, the Canadian Cancer Society and the Terry Fox Foundation, Genome Canada through the Ontario Genomics Institute, Ontario Institute for Cancer Research with funds from the province of Ontario, the Leukemia and Lymphoma Society, the Canadian Institutes for Health Research, a Canada Research Chair, and the American and Lebanese Syrian Associated Charities of St Jude Children's Research Hospital. This research was funded in part by the Ontario Ministry of Health and Long Term Care (OMOHLTC). The views expressed do not necessarily reflect those of the OMOHLTC.

Author Contributions F.N. designed study, analysed data and prepared figures. F.N., C.G.M., J.C.Y.W., A.P., S.D. and L.A.P. performed experiments. M.D.M. provided patient samples. J.C.Y.W. and M.D.M. provided patient outcome data. J.M. performed paired and unpaired segmentation analysis of SNP array data. F.N. and C.G.M analysed and interpreted SNP data. C.G.M., J.C.Y.W., S.D. and J.R.D. critically reviewed and edited the manuscript. F.N. and J.E.D. wrote the manuscript. J.E.D. supervised the study.

Author Information Reprints and permissions information is available at www.nature.com/reprints. The authors declare no competing financial interests. Readers are welcome to comment on the online version of this article at www.nature.com/nature. Correspondence and requests for materials should be addressed to J.E.D. (jdick@uhnres.utoronto.ca).

METHODS

Patient samples. Patient samples (primarily peripheral blood) were obtained from newly diagnosed Philadelphia-positive acute lymphoblastic leukaemia patients according to pre-established guidelines approved by the Research Ethics Board of University Health Network. Three out of twenty patient samples were donated by the Quebec Leukaemia Cell Bank. All samples were frozen viably using standard protocols in FCS + 10% DMSO and stored long term at −150 °C. Cell viability, as assessed immediately after thawing, was greater then 90% for all cases. Detailed patient data are provided in Supplementary Tables 6 and 7.

Xenotransplantation assay and analysis. NOD.CB17-*Prkdc*^{scid}/J (NOD/SCID) and NOD.Cg-*Prkdc*^{scid}*Il2rg*^{tm1Wjl}/SzJ (NSG) mice were bred according to protocols established and approved by the Animal Care Committee at University Health Network. Ten-to-twelve-week-old old mice were sublethally irradiated at 225 cGy 24 h before transplant. NOD/SCID mice were also treated with mouse anti-CD122 monoclonal antibody (NS122) after sublethal conditioning as previously described[20]. Only female mice were used in these studies[28]. NSG mice were periodically genotyped using standard PCR protocols (wild-type common forward primer, 5′-GTGGGTAGCCAGCTCTTCAG-3′; wild-type reverse, 5′-CCTGGAGC TGGACAACAAAT-3′; mutated reverse, 5′-GCCAGAGGCCACTTGTGTAG-3′). All primer sets were obtained from Jackson Laboratories website.

Frozen leukaemia cells were thawed by drop-wise addition of IMDM + 0.2 mg l^{-1} DNase (Roche Applied Science). After centrifugation, cells were resuspended in IMDM and counted using ViCell XR (Beckman coulter) or by trypan blue exclusion. For transplantation, cells were placed in microfuge tubes and spun down to remove excess media. Cells were resuspended in the correct volume (25 µl per mouse) for transplant using IMDM + 1% FCS. Intrafemoral transplant was performed as previously described[29]. Briefly, mice were anaesthetized using isoflurane. The right knee of mice was bent and drilled with a 27.5-g needle and followed by injection of cells with a 28.5-g insulin syringe (BD Biosciences).

After transplant, animals were monitored for the appearance of disease symptoms, such as weight loss, hunch-back, decreased activity, and killed soon after. Mice transplanted with samples that did not induce disease symptoms (in NS122 or NSG recipients) were killed by 16–24 weeks. Upon death, injected right femur (IF), non-injected bones (left femur, right and left tibiae, bone marrow (BM)), spleen and peripheral blood were removed and analysed for the presence of human leukaemia blasts using flow cytometry. Aliquots of cells were stained in 96-well round-bottomed plates (BD Falcon). Human cells were distinguished from mouse cells using human-specific CD45PC7 and CD44PE (Supplementary Fig. 18). B-cell-specific markers (various combinations of IgM FITC, CD19 PC5 (Beckman Coulter), CD20 APC7, CD10 APC, CD34 APC7) were used to evaluate blast phenotype after transplant. Detection of normal haematopoietic stem cell activity was monitored using CD33 PC5 (Beckman Coulter) or APC. T-cell engraftment in NSG mice was monitored using human CD3 FITC or APC. All fluorochromes were obtained from BD Biosciences unless otherwise indicated. Mice were considered to be engrafted when multiple human leukaemia markers (for example, $CD44^+CD45^+CD34^+CD19^+$) were detected by at least the 0.5% threshold. Virtually all cases of engraftment were well above this threshold. All flow cytometry analysis was performed on the LSRII (BD Biosciences). The remaining marrow (IF + BM) was frozen viably in FCS + 10% DMSO.

DNA SNP microarray analysis. DNA isolated from patients at diagnosis and xenograft samples was analysed using Affymetrix 6.0 SNP arrays. SNP array data were analysed using dChip no. 4 software using a reference algorithm and circular binary segmentation as previously described[11,18,19,30–32]. To distinguish inherited from somatic DNA copy number alterations for primary patient samples lacking matched normal DNA, putative variants identified by unpaired segmentation were filtered using public copy number polymorphism databases[33,34], and an in-house database of SNP array data from several hundred samples. SNP array data are available at dbGaP (phs000329.v1.p1) and is also hosted through St Jude Children's Research hospital (http://hospital.stjude.org/forms/genome-download/request/). Sample information is shown in Supplementary Table 7.

Quantitative PCR of the *CDKN2A/B* locus. Primers for genomic quantitative PCR were designed using Primer Express 3.0 (Applied Biosystems), and are listed in Supplementary Table 3. Taqman RNase P primers (Applied Biosystems) were used for control amplification. Fifty nanograms of leukaemic blast DNA or control human DNA was amplified using a 7500 Real-Time PCR system and 7500 System Software (Applied Biosystems), using the 7500 universal cycling conditions: 50 °C for 2 min, followed by 95 °C for 10 min, then 40 cycles of 95 °C for 1 min and 60 °C for 1 min. Standard curves for each *CDKN2A/B* exon and RNase P were generated using normal human DNA. Assays were performed in duplicate. *CDKN2A/B* exon-specific copy number values were normalized by dividing the value obtained for each test reaction by the paired value obtained for RNase P for each sample. Cutoffs of 0.65 and 0.3 were used to identify hemizygous and homozygous PAX5 deletions, respectively.

Statistical analysis. All data were analysed using GraphPad Prism version 5.00 for Mac OS X (http://www.graphpad.com). The Mann–Whitney *U*-test was used to assess statistically significant differences in chimaerism in xenografts. Clinical outcome data was analysed using the Gehan–Wilcoxon method based on random 10,000 permutations. Because the normal distribution of data can only be assumed in larger cohorts, this modified test more accurately computes *P*-values for small patient cohorts.

28. Notta, F., Doulatov, S. & Dick, J. E. Engraftment of human hematopoietic stem cells is more efficient in female NOD/SCID/IL-2Rgc-null recipients. *Blood* **115,** 3704–3707 (2010).
29. Mazurier, F., Doedens, M., Gan, O. I. & Dick, J. E. Rapid myeloerythroid repopulation after intrafemoral transplantation of NOD-SCID mice reveals a new class of human stem cells. *Nature Med.* **9,** 959–963 (2003).
30. Lin, M. *et al.* dChipSNP: significance curve and clustering of SNP-array-based loss-of-heterozygosity data. *Bioinformatics* **20,** 1233–1240 (2004).
31. Mullighan, C. G. *et al.* Genome-wide analysis of genetic alterations in acute lymphoblastic leukaemia. *Nature* **446,** 758–764 (2007).
32. Pounds, S. *et al.* Reference alignment of SNP microarray signals for copy number analysis of tumors. *Bioinformatics* **25,** 315–321 (2009).
33. Iafrate, A. J. *et al.* Detection of large-scale variation in the human genome. *Nature Genet.* **36,** 949–951 (2004).
34. McCarroll, S. A. *et al.* Integrated detection and population-genetic analysis of SNPs and copy number variation. *Nature Genet.* **40,** 1166–1174 (2008).

CORRECTIONS & AMENDMENTS

CORRIGENDUM

doi:10.1038/nature09877

Evolution of human *BCR–ABL1* lymphoblastic leukaemia-initiating cells

Faiyaz Notta, Charles G. Mullighan, Jean C. Y.Wang, Armando Poeppl, Sergei Doulatov, Letha A. Phillips, Jing Ma, Mark D. Minden, James R. Downing & John E. Dick

Nature **469,** 362–367 (2011)

On page 2 of the PDF and print version of this Article, column one, under the heading 'Genetic basis of functional heterogeneity', line 9 should refer to Fig. 1e instead of Fig. 2e. Similarly, in column two of the same section, lines 7 and 9 should ref to Fig. 1f and 1g, respectively, instead of Fig. 2f and 2g. These have now been corrected in the HTML version of the manuscript.